REPORT No. 792

FLIGHT STUDIES OF THE HORIZONTAL-TAIL LOADS EXPERIENCED BY A FIGHTER AIRPLANE IN ABRUPT MANEUVERS

By Flight Research Maneuvers Section

SUMMARY

Flight measurements were made on a fighter airplane to determine the approximate magnitude of the horizontal tail loads in accelerated flight. In these flight measurements, pressures at a few points were used as an index of the tail loads by correlating these pressures with complete pressure-distribution data obtained in the NACA full-scale tunnel. In addition, strain gages and motion pictures of tail deflections were used to explore the general nature and order of magnitude of the fluctuating tail loads in accelerated stalls.

The results indicated that, if the airplane were not stalled, a total up load of 5700 pounds would be experienced on the horizontal tail in an 8g pull-up and that, with power on, this load would be distributed unsymmetrically with about 800 pounds more up load on the left stabilizer than on the right. When stalling occurred there was an initial abrupt increase in the up tail load of the order of 100 percent of the previous load, which was followed by repeated load and stress variations due to tail buffeting. Under the conditions of tail buffeting, the possibility of excessive stresses due to resonance was indicated.

INTRODUCTION

As a result of numerous tail failures of high-speed airplanes in flight, a flight investigation was undertaken to determine the general nature of horizontal tail loads experienced in abrupt pull-up maneuvers. Tests were made by the NACA at Langley Field, Va., during the spring and summer of 1942. The flight-test procedure involved the use of pressure measurements made at a few points on the horizontal tail, which were correlated with complete pressure-distribution data from the NACA full-scale tunnel to determine the approximate tail loads. This procedure gave satisfactory results except when applied to stalls wherein abnormally high fluctuating pressures, corresponding to tail buffeting, were experienced. In order to help establish the significance of the peak pressures recorded, a strain gage capable of following the load fluctuations was installed on the stabilizer; motion-picture cameras were installed later to record the deflection of the horizontal-tail surfaces.

The results of the tail-load measurements obtained are discussed in two main parts. One part pertains to the more or less steady loads experienced in maneuvers, for which the determination of loads by means of the measured pressures is fairly straightforward. The second part deals with the fluctuating loads experienced in stalled flight wherein the significance of the measured pressures was difficult to establish. For this second case, the main dependence is placed on strain measurements and photographs of the tail deflections.

DESCRIPTION OF AIRPLANE AND APPARATUS

Test airplane.—The tail-load tests were made on a fighter airplane having the plan form and dimensions shown in figure 1. The gross weight of the airplane was maintained between 11,900 pounds and 12,000 pounds for the tests. The center-of-gravity position was maintained between 29.8 percent and 30.2 percent mean aerodynamic chord.

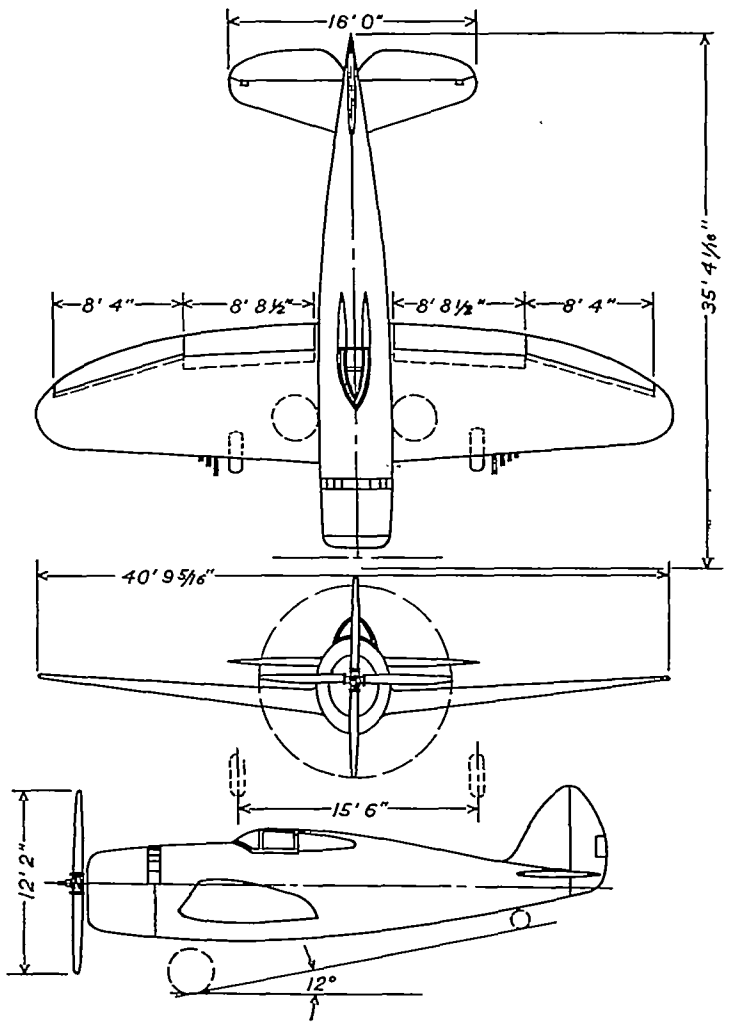

Figure 1.—Three view drawing of airplane.

Basic flight instruments.—Airspeed, elevator angle, stick force, and normal acceleration were recorded during the tests by standard NACA recording instruments. The airspeed recorder was connected to an NACA swiveling static head located 1 chord length ahead of the right wing tip and to a shielded total head mounted on the airspeed boom.

Pressure-orifice installation.—Four pairs of orifices were installed on the horizontal stabilizer to measure the pressure difference between the upper and lower surfaces of the stabilizer. The spanwise and chordwise locations of the orifices were chosen to correspond with particular orifices used in the pressure-distribution measurements made in the NACA full-scale tunnel. A sketch showing the location of the orifices used in the flight tests is given in figure 2. Pressures were recorded for the individual orifices by an NACA mechanical manometer mounted in the baggage compartment of the

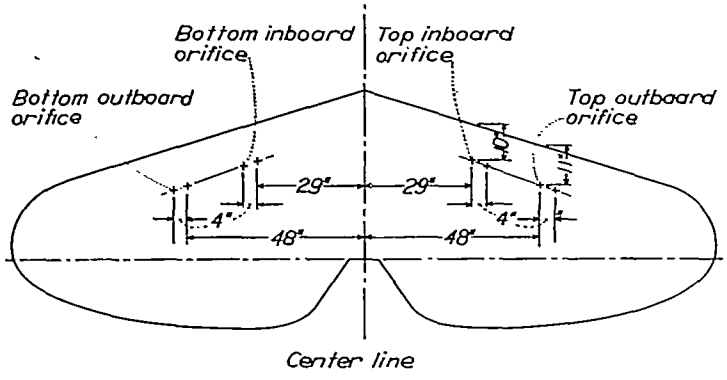

FIGURE 2.—Horizontal tail showing pressure-orifice locations.

airplane. The inboard orifices were connected to high-frequency pressure recorders to permit a study of the pressure fluctuations at the stall.

Tail-deflection apparatus.—The deflections of the horizontal tail under load were measured by photographing the tail with two 16-millimeter motion-picture cameras mounted, one on each side of the fuselage, in the intercooler exit ducts. The cameras were synchronized by timing lights operated by a master timer that also synchronized all the recording instruments in the airplane. Targets were painted on the tail plane to identify the spanwise position in the photographic records. The camera installation and the targets on the horizontal tail are shown by photographs in figures 3(a) and 3 (b), respectively.

Strain-gage installation.—An electrical strain gage was installed on the skin above the rear spar on the right horizontal stabilizer. A photograph showing the location of the strain gage and the dummy gage on the horizontal tail is given in figure 4. The orifices on the upper surface of the

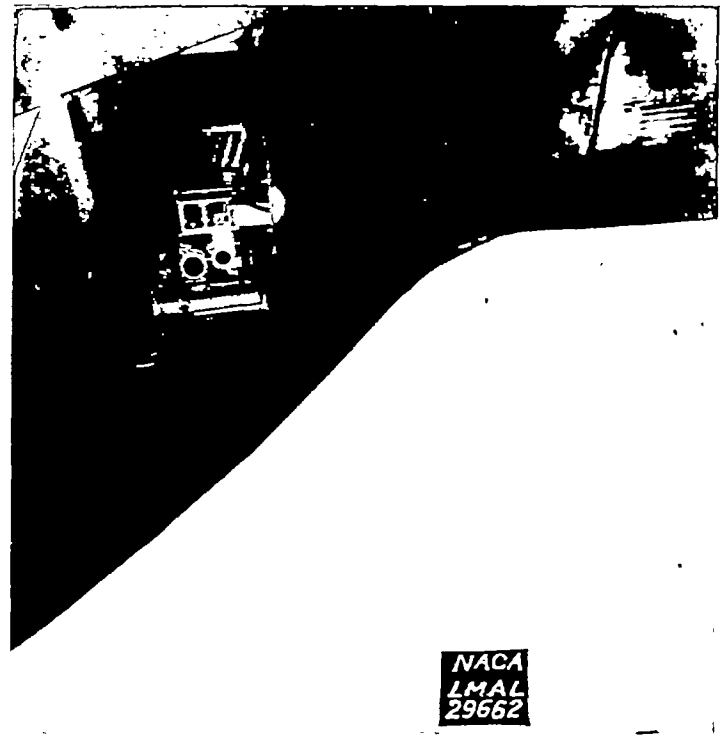

(a) Camera mounted in intercooler exit.

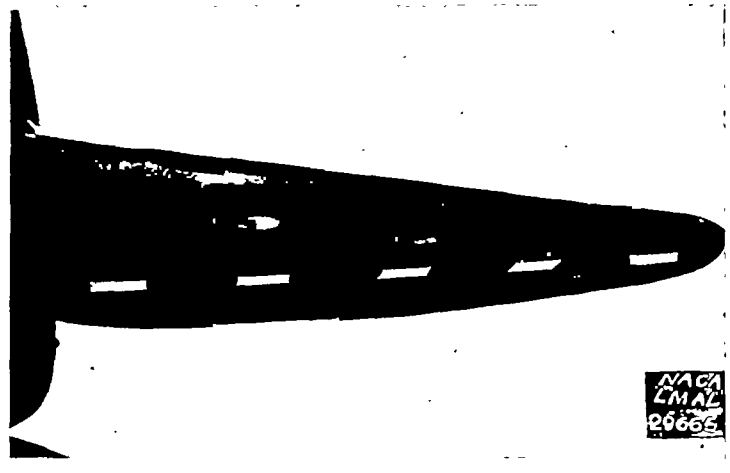

(b) Targets painted on left stabilizer.

FIGURE 3.—Installation for photographing tail deflections.

tail and the leads from the orifices on the lower surface are also shown in figure 4.

For one flight, de Forest scratch-type strain gages were mounted along the front spar on the upper skin of the left stabilizer at 34, 60, and 74.5 inches from the stabilizer tip. The gages were mounted by gluing the gage target and scratch arm to the skin.

TEST PROCEDURE

The types of tests and records obtained are summarized in the following table:

Flight	Type of maneuver	Records obtained			
		Basic flight	Pressure distribution	Strain gage	Tail deflection
14B	Abrupt pull-ups	Yes	Yes	No	No
15B	Abrupt pull-ups	Yes	Yes	No	No
18B	Abrupt pull-ups	Yes	Yes	Yes	No
19B	180° turns	Yes	Yes	Yes	No
21B	Abrupt pull-ups and 180° turn	Yes	Yes	Yes	Yes
24B	Abrupt pull-ups	Yes	Yes	Yes	Yes

It is apparent from the table that the test program progressed from an installation that measured only pressures on the horizontal tail to one consisting of a combination of pressure orifices and a strain gage and, finally, to an installation which simultaneously measured the pressure, strain, and tail deflection. The strain gage was installed to facilitate an interpretation of the pressure fluctuations experienced on the horizontal tail at and beyond maximum lift of the wing in the pull-ups. The apparatus for measuring tail deflection was subsequently added in an effort to obtain additional data on the motion of the tail following the wing stall for correlation with the pressure fluctuations and the strain measurements.

The abrupt pull-ups to maximum lift were made at various speeds, from the minimum speed of the airplane to an indicated airspeed of approximately 214 miles per hour. The corresponding normal accelerations experienced ranged from $1g$ to $4.5g$. All tests were made at an altitude of approximately 6000 feet and, except for one power-off run, with the engine operating at 2450 rpm and 27 inches of mercury manifold pressure.

DETERMINATION OF TAIL LOADS

The pressure data recorded in flight were converted to tail loads from the pressure-distribution data for the tail plane obtained in the NACA full-scale tunnel. Because of an unsymmetrical flow in the full-scale-tunnel tests, the load on the tail, as indicated by integration of the measured pressures, was unsymmetrical. The dissymmetry of load is shown in figure 5, which is a plot of the spanwise distribution of load on the horizontal tail. The variable $c_n c$ used in this figure is the product of the section normal-force coefficient c_n and the local chord c.

The normal-force coefficients C_N for each half of the tail were plotted in figure 6 as a function of the pressure coefficient $\Delta p/q$, in which Δp is the difference between the pressures on the upper and lower surfaces of the tail plane at the two spanwise stations where orifices were located in the flight-test installation and q is the dynamic pressure. The tail loads computed from pressures measured at the individual orifices therefore assume a symmetrical tail load with a load distribution similar to that obtained in the full-scale-tunnel tests. The normal-force coefficients for the tail are noted to be pro-

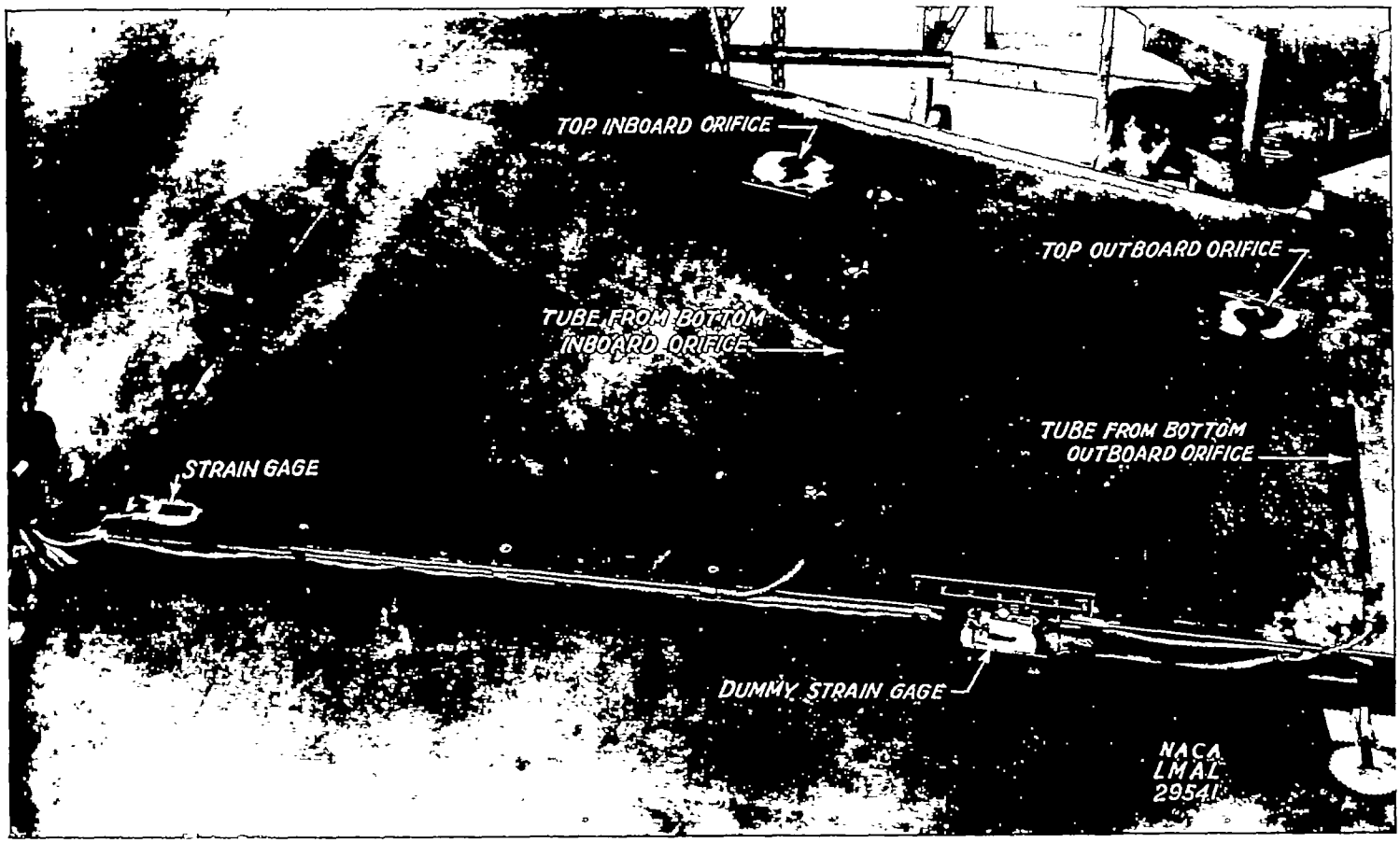

FIGURE 4.—Photograph of pressure orifice and strain-gage installation on top surface of right stabilizer.

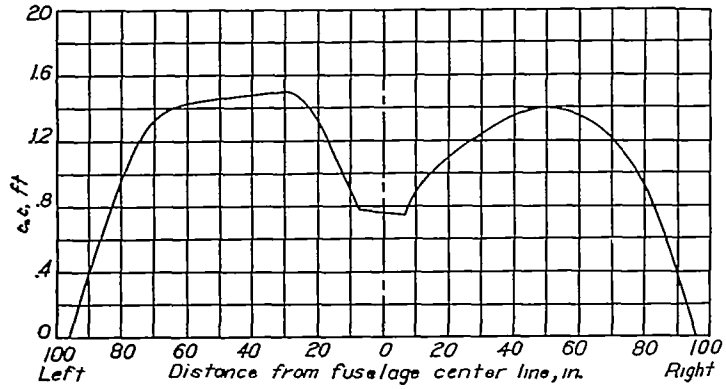

FIGURE 5.—Spanwise load distribution obtained from pressure-distribution tests in NACA full-scale tunnel.

portional to the pressure difference across the tail plane and are also a function of the elevator angle δ_e. The tunnel data for the right inboard orifice were considered too inconsistent for use in evaluating the tail loads (see fig. 6) and the evaluation of tail loads for the flight tests was therefore based on measurements at the other three stations.

Tail loads were determined from the tail-deflection data by means of the influence line shown in figure 7 and the spanwise load distribution of figure 5. The influence line

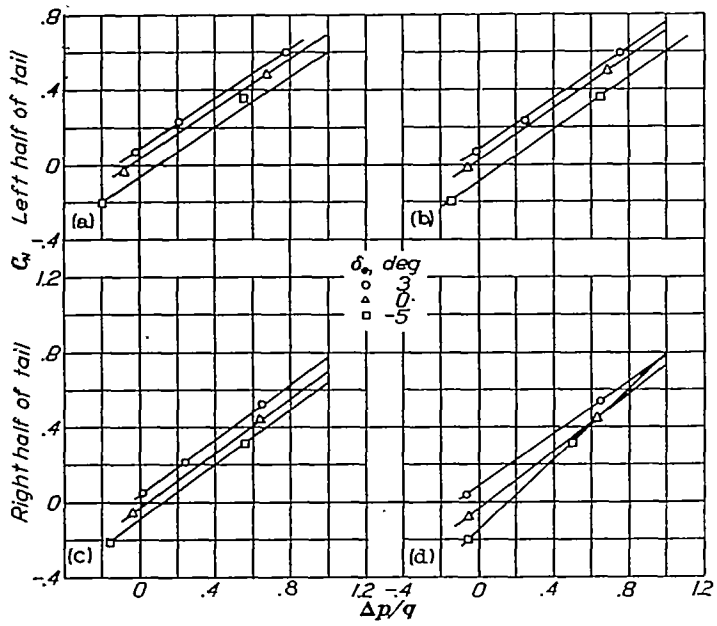

(a) Left outboard orifice. (b) Left inboard orifice.

(c) Right outboard orifice. (d) Right inboard orifice.

FIGURE 6.—Calibration of orifices from full-scale-tunnel tests.

was obtained exerimentally by applying unit up loads at the indicated spanwise points, whereas the spanwise load distribution was taken from NACA full-scale-tunnel data. The tail load per inch stabilizer deflection is obtained by the summation

$$\sum_{0}^{b/2} yw\,\Delta b$$

in which w is the running load at a spanwise point, y is the ordinate of the influence line at the same point, and b is the span of the horizontal tail. This summation shows a

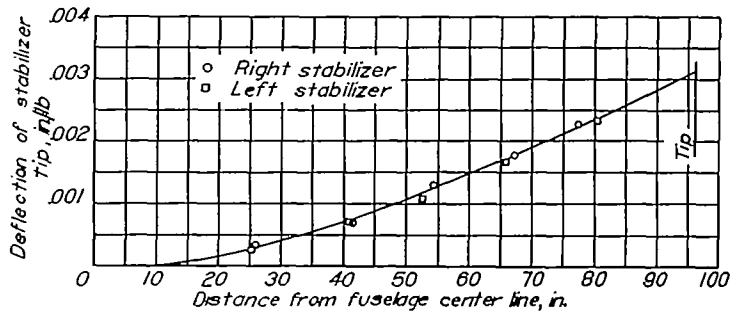

FIGURE 7.—Influence line of stabilizer-tip deflection.

load of 875 pounds per inch tip deflection on the right stabilizer and 976 pounds per inch tip deflection on the left stabilizer.

Some question may be raised as to how the spanwise load distribution (fig. 5) should be faired across the fuselage, but consideration of possible changes would not materially alter the loads as measured by tip deflection.

RESULTS AND DISCUSSION

Loads in unstalled flight.—The tail loads in accelerated flight were measured in pull-ups to maximum lift of the wing. Time histories of airspeed, normal acceleration, elevator position, and elevator stick force for three typical pull-ups of varying acceleration are presented in figure 8. The present discussion is limited to the loads attained before the wing stalled, that is, to the portion of the maneuver prior to tail buffeting, as is indicated by the fluctuating normal-acceleration curve.

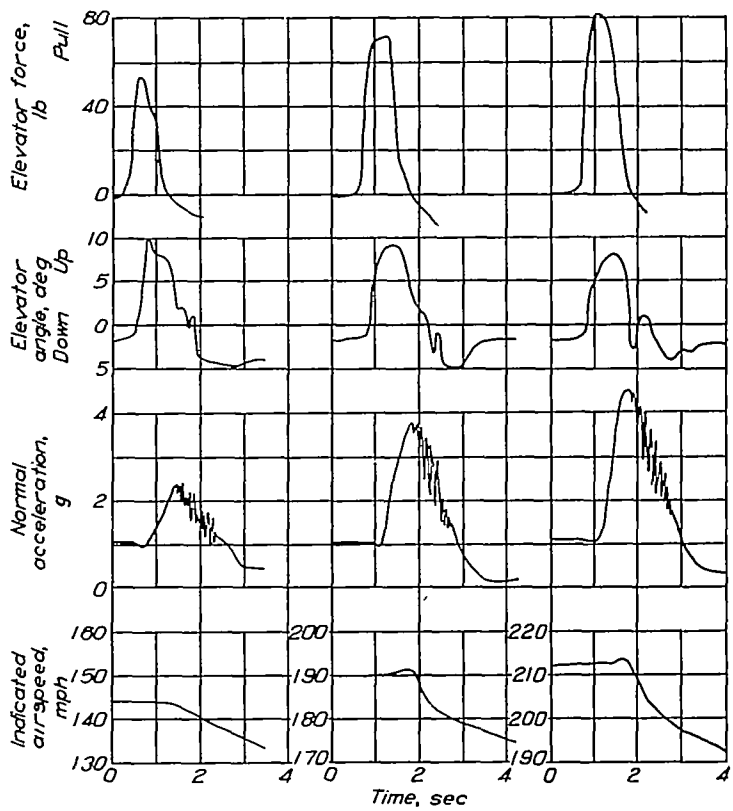

FIGURE 8.—Time histories of pull-ups to maximum lift. Power on; manifold pressure, 27 inches of mercury at 2450 rpm; center of gravity, 29.8 percent M. A. C.

The pressure coefficients $\Delta p/q$ for the four spanwise points are listed in table I. The corresponding values of normal-force coefficient C_N obtained by reference to figure 6 are also listed for the three stations at which satisfactory calibrations were available. Total tail loads corresponding to the normal-force coefficients of table I (tail load equals $55qC_N$) have been plotted in figure 9 as a function of normal acceleration. Extrapolating these data indicates that an up

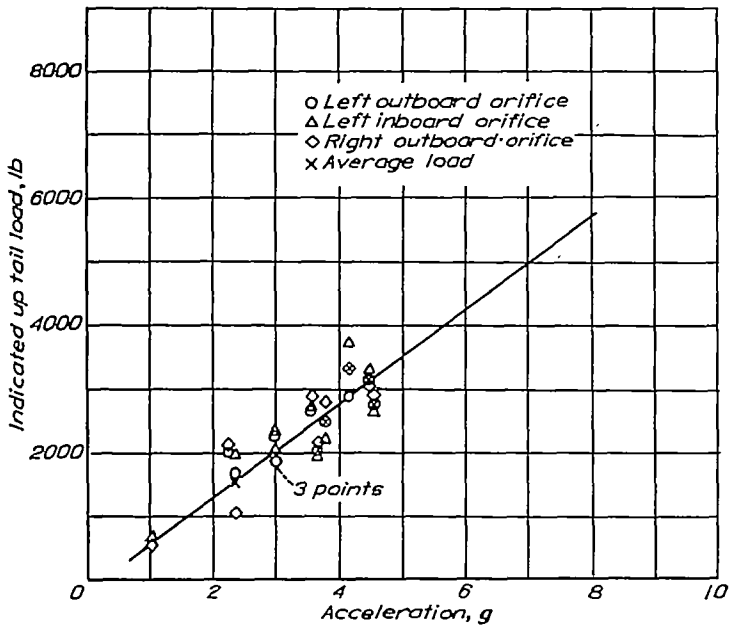

FIGURE 9.—Tail loads before wing stalled, computed from pressure-orifice measurements in pull-ups to maximum lift.

load of about 5700 pounds would be experienced at an acceleration of $8g$.

In consideration of these tail loads, a study was made to learn the contribution to the load of each of the following factors:

(a) Increment of tail load necessary to balance pitching moment of wing-fuselage-propeller combination

(b) Increment of tail load due to horizontal location of center of gravity with respect to aerodynamic center of wing-fuselage-propeller combination

(c) Increment of tail load due to manipulation of elevator

At the speeds investigated, the increment of tail load due to factor (a) (a down load) was found to be relatively small, about $5.5q$ or 560 pounds at 200 miles per hour. At diving speeds, however, this increment is large enough to be of primary consideration.

The increment of tail load due to factor (b) is always an up load at positive lifts with the conventional wing and tail arrangement; if the aerodynamic center of the wing-fuselage-propeller combination is known, determining this increment of tail load for any center-of-gravity position, gross weight, and normal acceleration resolves into a simple moment problem. The increment of tail load varies directly as the product of the gross weight and normal acceleration and varies linearly with center-of-gravity location; that is, this increment of tail load will be zero for every flight condition if the center of gravity and aerodynamic center are coincident and will increase as the center of gravity moves rearward.

Full-scale-tunnel tests indicate that the aerodynamic center of the fuselage-wing-propeller combination (power on) of the airplane tested is at approximately 15 percent of the mean aerodynamic chord. With this aerodynamic center, the increments of tail load calculated by the method suggested are in substantial agreement with tail loads obtained from flight-test data. The tail loads experienced during acceleration were considerably larger than the loads indicated by standard design practice because the propeller and fuselage caused the aerodynamic center to move farther forward than had been anticipated.

A discussion of the effect on the tail loads of factor (c) (elevator manipulation) requires a knowledge of the control movement during the maneuver. It is apparent from figure 8 that the elevator force is relaxed before the maximum acceleration is reached and as a result the stick force is approximately zero at the time of maximum acceleration. When the elevator stick force is zero, the elevator is floating, and the tail-load increment due to a combination of factors (b) and (c) is equal to that obtained in a similar maneuver, elevator fixed, with the center of gravity at the point giving zero stick-free stability. Computed on this basis, the up tail load due to releasing the elevator is 130 pounds per g of normal acceleration. Extrapolation of the data in figure 10, which is discussed subsequently, corroborates experimentally this calculated load increment. This load increment is indicated by the difference between the curves shown for elevator floating and elevator fixed as determined from unstalled pull-ups and steady turns, respectively.

Pull-ups to maximum lift and unstalled pull-ups to the same acceleration gave dissimilar tail-loading conditions. Analysis of the data indicates that the load was unequally distributed between the right and left stabilizers during unstalled pull-ups, as shown in figure 10. The total tail load, however, was the same as that obtained in pull-ups to maximum lift. (Compare $4.5g$ pull-ups in figs. 9 and 10.)

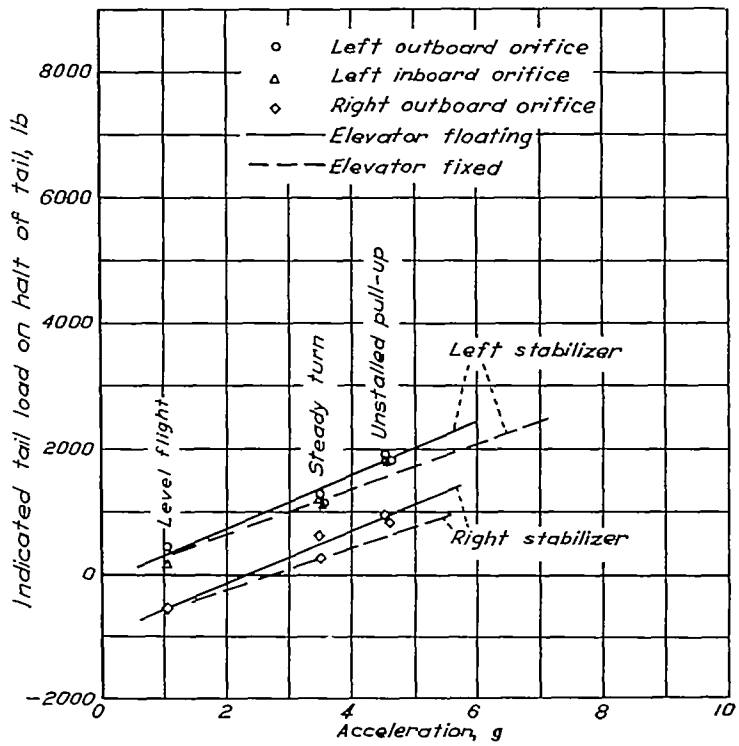

FIGURE 10.—Unsymmetrical spanwise loading indicated by pressure-orifice measurements.

A clue to the probable cause of the asymmetric load is obtained by a study of the time histories of figures 11 and 12. A turn with power on is shown in figure 11. Immediately before this turn was entered, the load on the left stabilizer was greater than that on the right stabilizer and remained greater by about the same amount throughout the turn. The pressure changes that occurred during the turn were very similar on both sides of the tail and occurred simultaneously with acceleration changes. For the turn of figure 12, which was executed with power off, the loads were nearly equal on both stabilizers, with the pressure orifices indicating a slightly larger tail load on the right stabilizer. The changes in pressure during this turn were similar to the changes that occurred in the power-on turn. Consideration of the magnitude of the dissymmetry in loading indicates that the unsymmetrical tail loading is attributable to a slipstream twist which increases the angle of attack on the left stabilizer 2° or 3° in a positive direction and decreases the angle of attack on the right stabilizer by an equal amount.

It appears from these data that the slipstream twist with power on is responsible for an asymmetric tail-load increment except at maximum lift. (See fig. 9.) The dissymmetry, which is independent of speed and acceleration, results in an up load on the left stabilizer 800 pounds greater than that on the right stabilizer. This unsymmetrical loading, if attained in an accelerated pull-up of 8*g*, would result in a tail load of 3250 pounds on the left half of the tail or in a stress due to an equivalent uniform tail load of 6500 pounds.

Loads during stalled flight.—In abrupt pull-ups to maximum lift, large and erratic tail-load increments were indicated by sharp pressure rises immediately after the stall occurred. The initial peak pressures were followed by fluctuating pressures throughout the period of stalled flight. Time histories of pull-ups to maximum lift (figs. 13 and 14) show the nature of these pressure rises and fluctuations, together with simultaneous records of strain as indicated by the electrical strain gage. These abrupt pressure rises and fluctuations are ascribed to fluctuations in direction of the air flow at the tail, which are due to stalling of the wing.

As was previously mentioned, cameras were installed to record the motion of the horizontal tail during pull-ups. The accuracy of measurements of leading-edge deflections on the 16-millimeter film is believed to be within ±0.0005 inch, which is equivalent to ±0.1 inch of actual tail deflection. Although a camera speed of approximately 64 frames per second was used, the frequency of the tail vibrations was such that the maximum amplitude of the motion of the tail was not necessarily defined. The data were therefore plotted (figs. 15, 16, and 17) in the form of instantaneous beam-deflection diagrams at time increments of approximately 0.017 second during the stalled part of the pull-up. In these figures, if a line faired through the spanwise points at which deflections were measured did not pass through zero deflection at the center line of the tail (see 2.500 seconds, fig. 15), the beam diagram was arbitrarily shifted so that the deflection at the center line was zero. The shifted beam curves appear in the figures as dashed lines. This shift of the beam curve is considered justifiable on the basis that vibration in the airplane may have caused slight shifting of the cameras or that the zero reading for the particular frame may have been in error; either of these factors would have caused a uniform shift of the beam line. The change in tail load, which is indicated by the deflection of each stabilizer tip, is listed at the end of each beam curve. In figures 16 and 17, the total load change for each beam diagram is tabulated at the center line. Deflections of the stabilizer are also plotted as time histories, together with airspeed, acceleration, pressure, and electrical strain-gage records in figures 18 to 20. A marked twisting action of the fuselage may be noted during the stalled portion of the pull-ups. The deflections of the right- and left-stabilizer tips are not, therefore, a reliable indication of the individual loads developed on the right and left stabilizers except during the first part of the maneuvers before the twisting of the fuselage was set up. The axes for the pressure and electric strain-gage records were so drawn that the ordinates at the beginning of the run and at the time of maximum acceleration are proportional to the loads computed at these points. Because both the electric strain gage and the pressure capsule have straight-line calibrations, succeeding peaks are also proportional to the tail load.

The three de Forest strain gages mounted on the left stabilizer provided a measure of stress on the upper skin of the left stabilizer during the runs of figures 16 and 17. The de Forest strain-gage records are shown in figure 21 and a photomicrograph of a typical record is shown in figure 22. Although a history of the stress encountered was recorded by a de Forest scratch gage, no time record is available. The peak stresses, therefore, do not indicate the frequency of the applied load and must be interpreted in conjunction with other records.

The change in load from the level-flight condition to the point of maximum acceleration that occurred immediately before the stall is indicated by ΔL_1 in figure 13 and the change in load indicated by the first peak on the pressure or strain-gage record after the stall occurred is indicated by ΔL_2. The ratios of the load immediately after the stall to the load before the stall $\Delta L_2/\Delta L_1$ as indicated by pressure-orifice and electric-strain-gage records, as well as similar ratios determined from the tip-deflection and de Forest strain-gage records, are listed in the following table:

Figure	Load ratio, $\Delta L_2/\Delta L_1$							
	Pressure orifice		Electrical strain gage (root of right stabilizer)	Tip deflection		de Forest strain gages, from left tip		
	Right inboard	Left inboard		Right tip	Left tip	74 in.	60 in.	34 in.
13	1.5	1.9	2.4	-----	-----	-----	-----	-----
14	1.5	2.6	1.8	-----	-----	-----	-----	-----
18	1.1	-----	1.4	-----	2.0	-----	-----	-----
19, 21	1.2	2.6	1.6	1.8	1.0	1.5	1.0	1.8
20, 21	1.3	1.4	1.5	1.5	1.1	1.0	1.3	1.3

The tabulated data show that immediately after the stall a large and abrupt increase in the up tail load occurred.

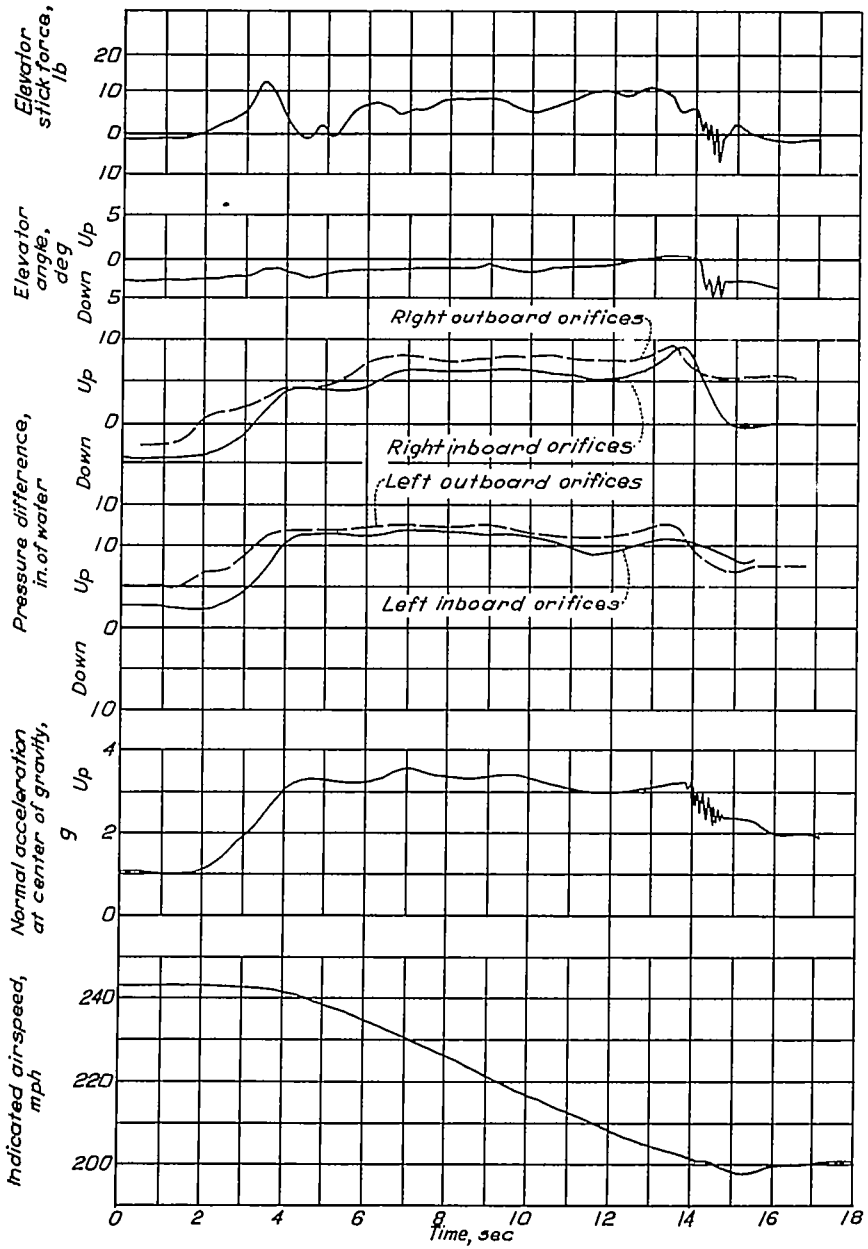

FIGURE 11.—Time history of 180° left turn. Power on; manifold pressure, 30 inches of mercury at 2450 rpm. Note dissymmetry of pressures on left and right stabilizers.

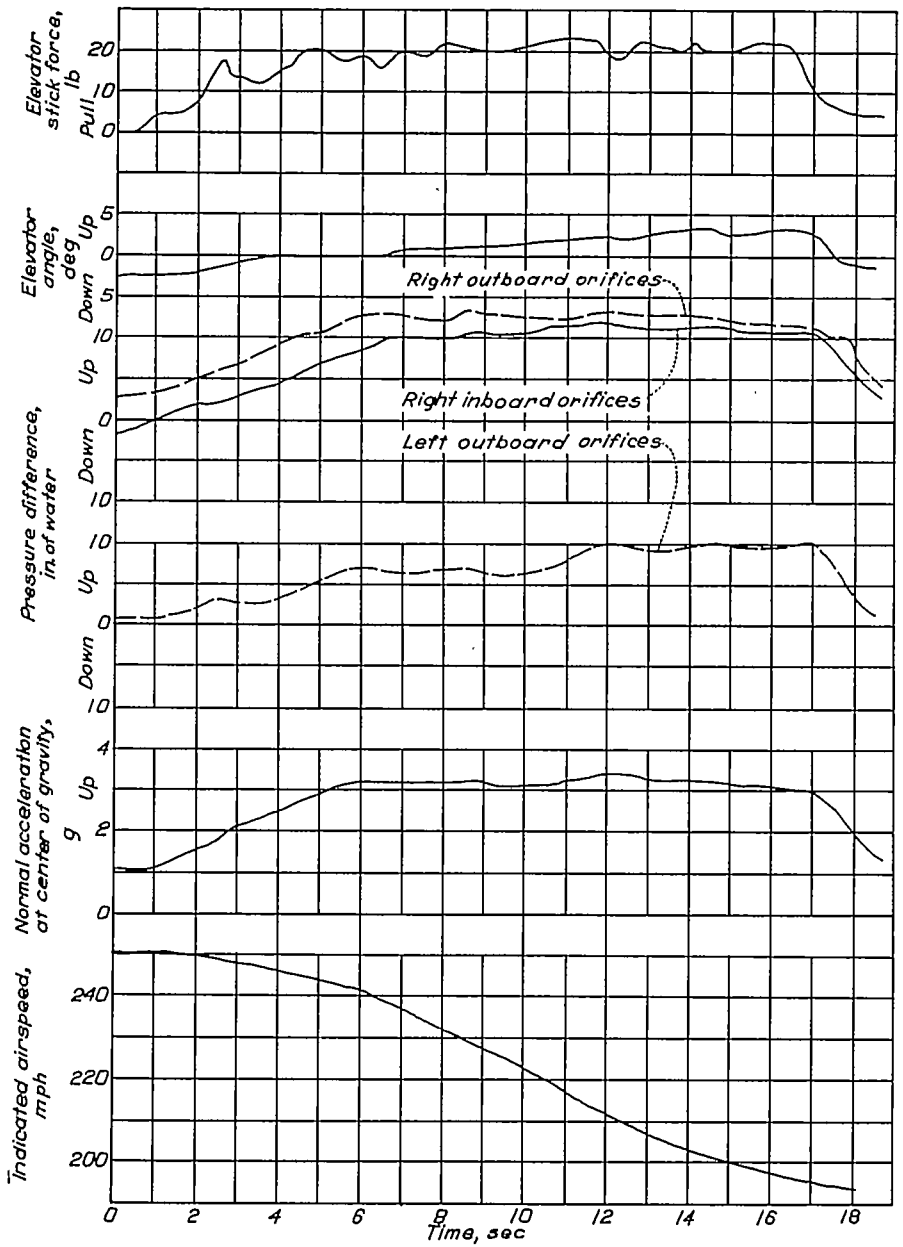

FIGURE 12.—Time history of 180° left turn. Power off. Note that pressures on right stabilizer are slightly greater than on left stabilizer.

Although changes in load indicated by each of the records obtained are listed in this table, the indications of the pressure orifices are discounted, not only because of uncertainty regarding the dynamic characteristics of the pressure-recording system, but also because of uncertainty regarding the applicability of point pressures in relation to total loads under these circumstances. The fact should also be noted that, owing to the inertia of the tail structure, momentary pressure increments would not necessarily result in comparable stress increments. The strain-gage and deflection measurements indicate that the initial effect of the stall may result in up loads of the order of twice those loads experienced immediately prior to stalling.

After the initial tail-load increment occurs because of wing stalling, the tail is buffeted repeatedly by the fluctuating downwash in the turbulent wake from the stalled wing. The possibility for resonance between the turbulence frequency and certain natural frequencies of the tail structure exists under this condition. The frequency of the horizontal tail in primary bending was 17½ cycles per second and the frequency of the complete tail in torsion of the fuselage was 10 cycles per second. From tests in the NACA full-scale tunnel, the frequency of the turbulence fluctuations from the stalled wing was found to be 5.5 cycles per second at 65 miles per hour. If this frequency were a linear function of true airspeed, the range would be from about 13 to 20 cycles per second in the speed range covered by the pull-up tests and, at some speeds, would coincide with the bending frequency of the tail. The turbulence frequencies, however, as shown by the pressure records taken at the tail, were seldom actually uniform for more than 2 or 3 cycles. Moreover, where definite frequencies were detectable, the turbulence frequencies appeared to range from about 10 to 35 cycles per second and to be independent of the speed of flight. This lack of regularity in the turbulence pattern was not unexpected because both the angle of attack of the wing and the position of the tail in the wing wake were rapidly varying with time. In two of the pull-up maneuvers, however, resonance with the tail structure occurred when pressure fluctuations of a frequency close to that of the tail were sustained for several cycles. An example of this condition of resonance is shown by the pull-up recorded in figure 14 where a large periodic build-up in stress occurred as a result of a series of regular pressure fluctuations. Figure 13 shows a somewhat similar condition at a different airspeed. Both records clearly indicate the mechanism by which excessive tail stresses can be produced when tail buffeting occurs.

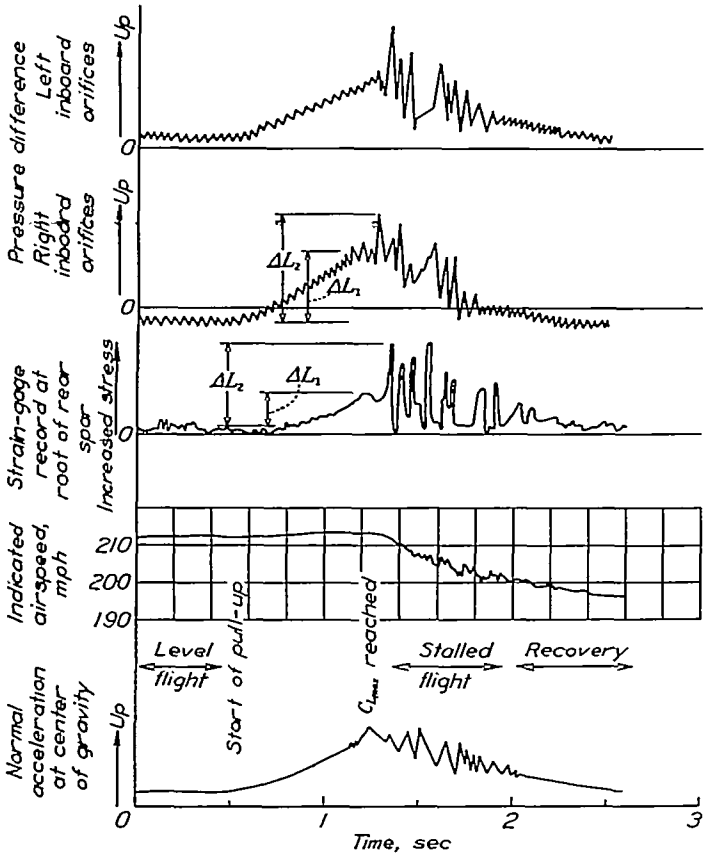

FIGURE 13.—Time history of a rapid 4.5g pull-up to maximum lift at 212 miles per hour.

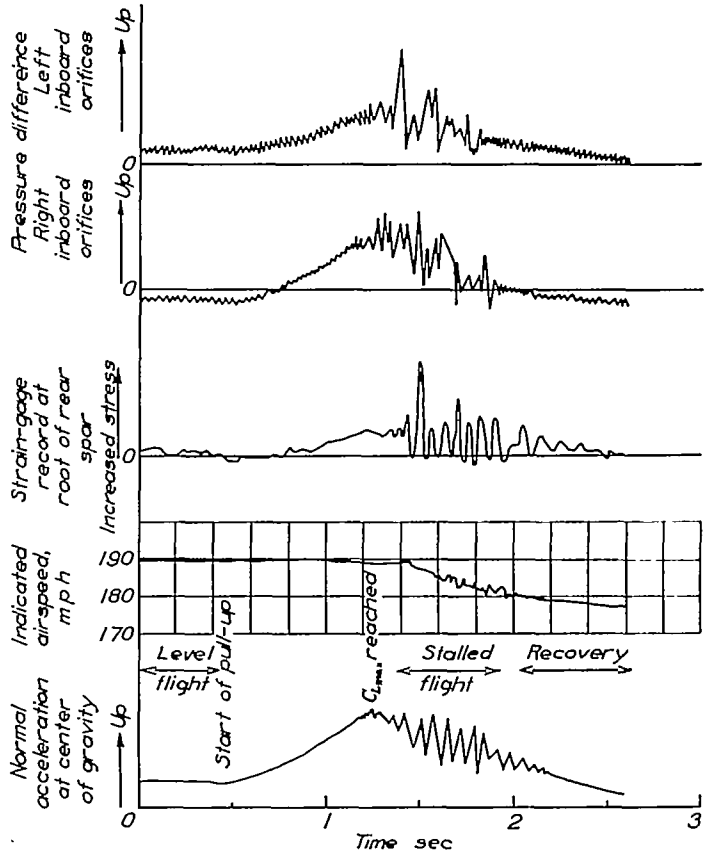

FIGURE 14.—Time history of a rapid 3.8g pull-up to maximum lift at 190 miles per hour.

CONCLUSIONS

The results of the present tail-load tests with a fighter airplane show the type and the general magnitudes of loadings encountered on the horizontal tail of a heavily loaded fighter airplane in accelerated maneuvers. The survey of critical conditions is not complete, however, because no tests were made in the high-speed and diving-speed ranges. In addition, the measurements that were obtained are less complete and less detailed than are required to present an accurate quantitative picture of the loads, particularly the loads immediately after the stall and during tail buffeting. The need for further investigation of these conditions is indicated

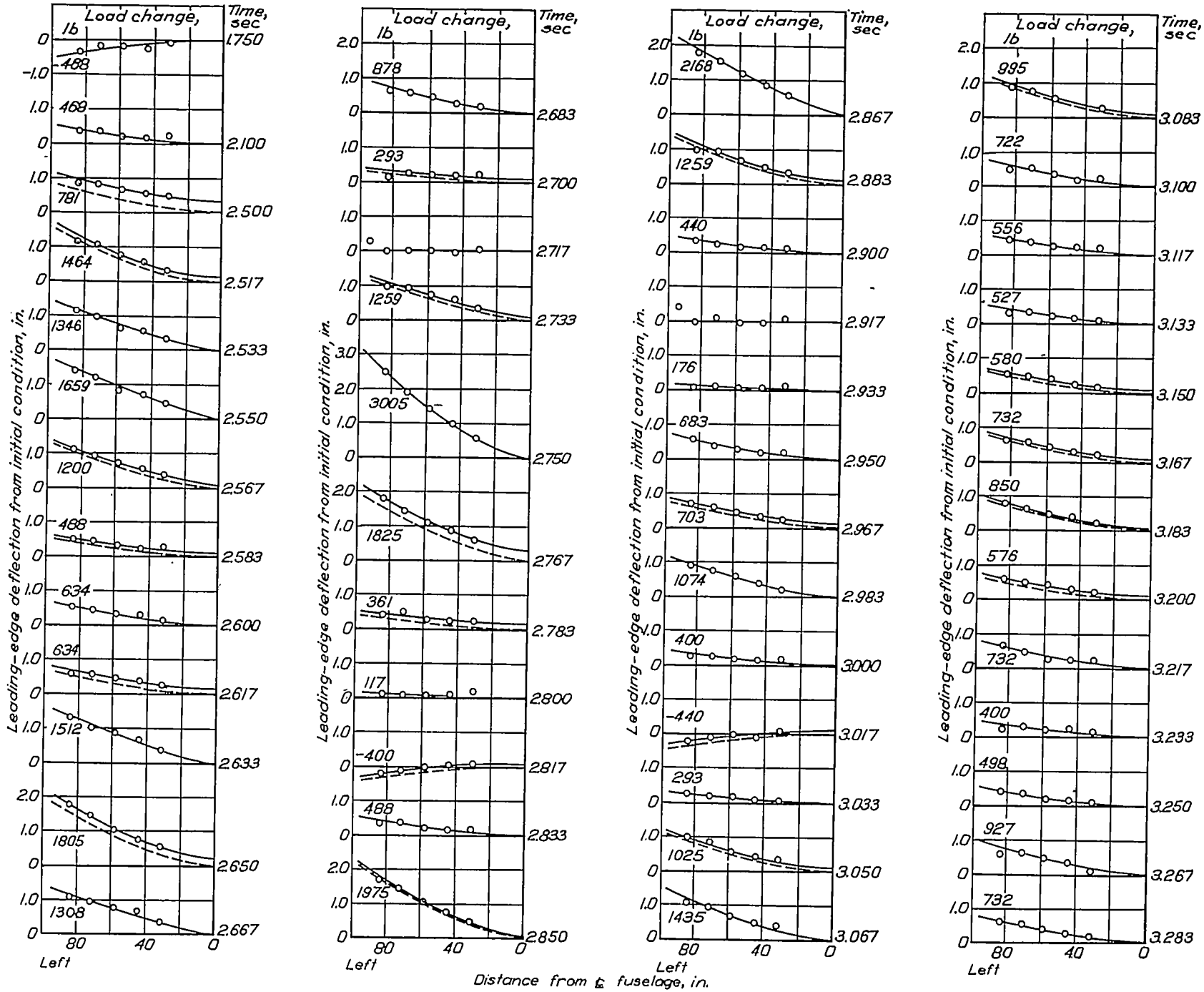

FIGURE 15.—Instantaneous beam diagrams of left stabilizer during a 4.2g pull-up to maximum lift. Run 1 of flight 21B.

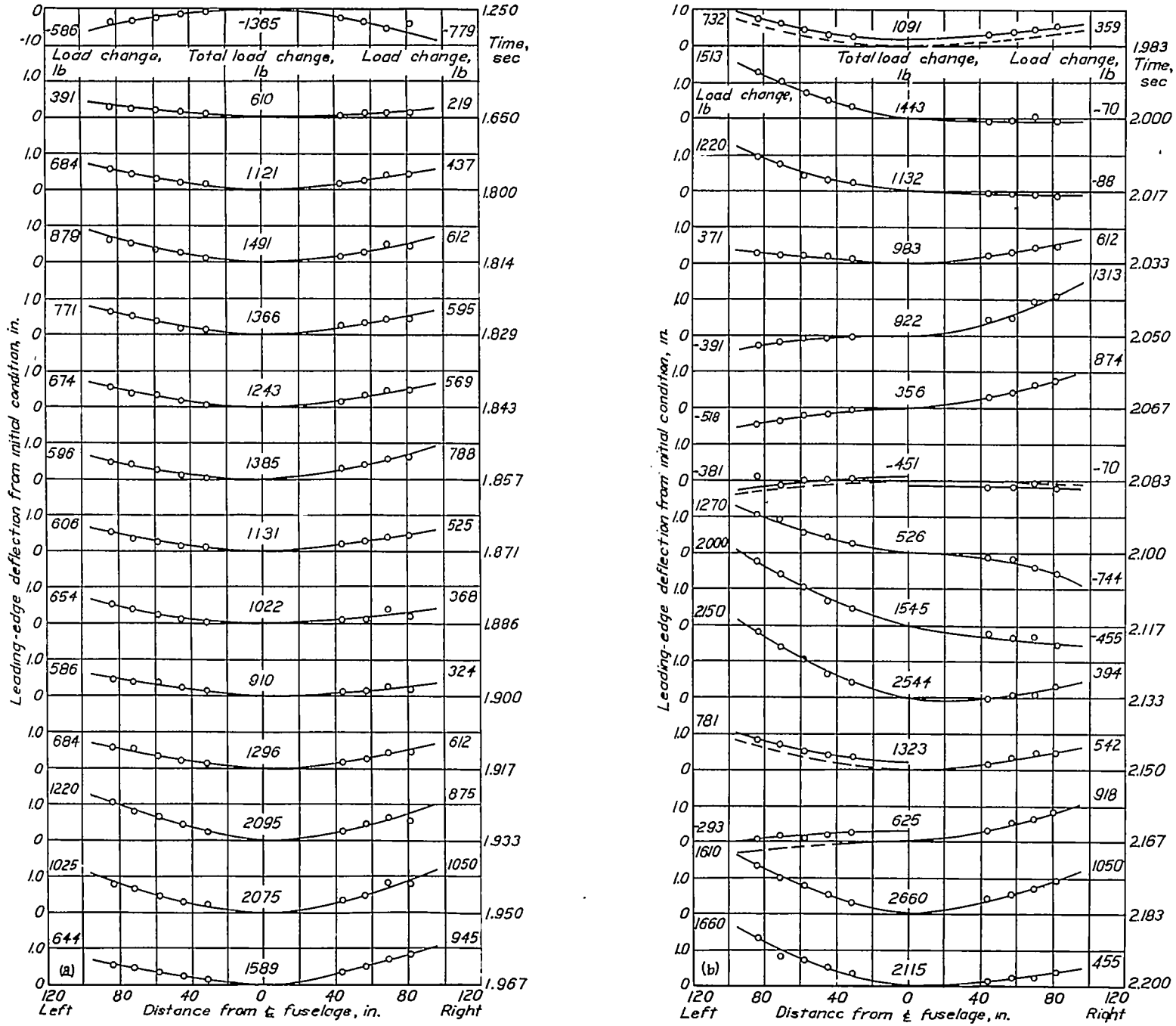

FIGURE 10.—Instantaneous beam diagrams of stabilizer obtained during a 2.4g pull-up to maximum lift. Run 1 of flight 24B.

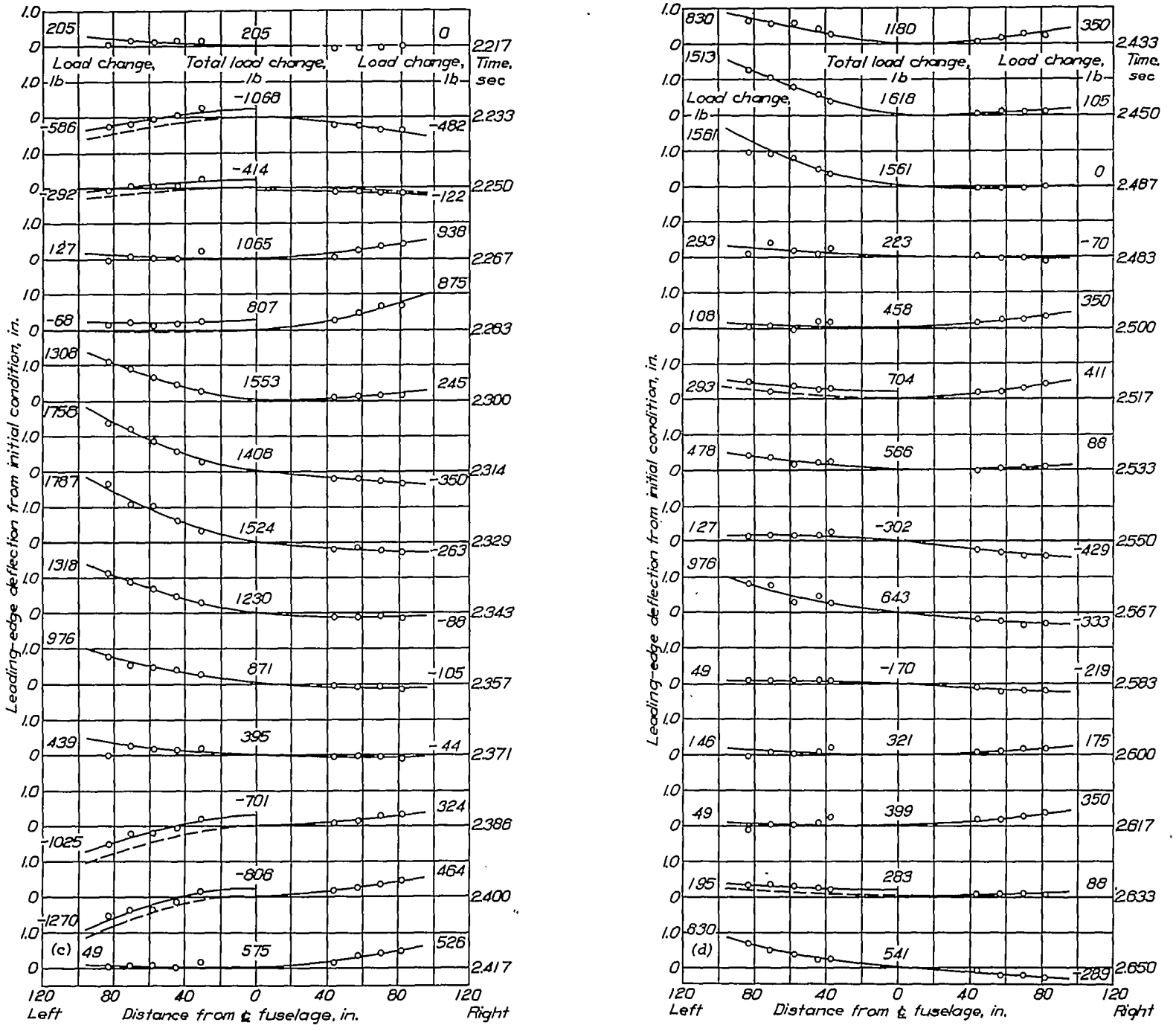

FIGURE 16.—Concluded.

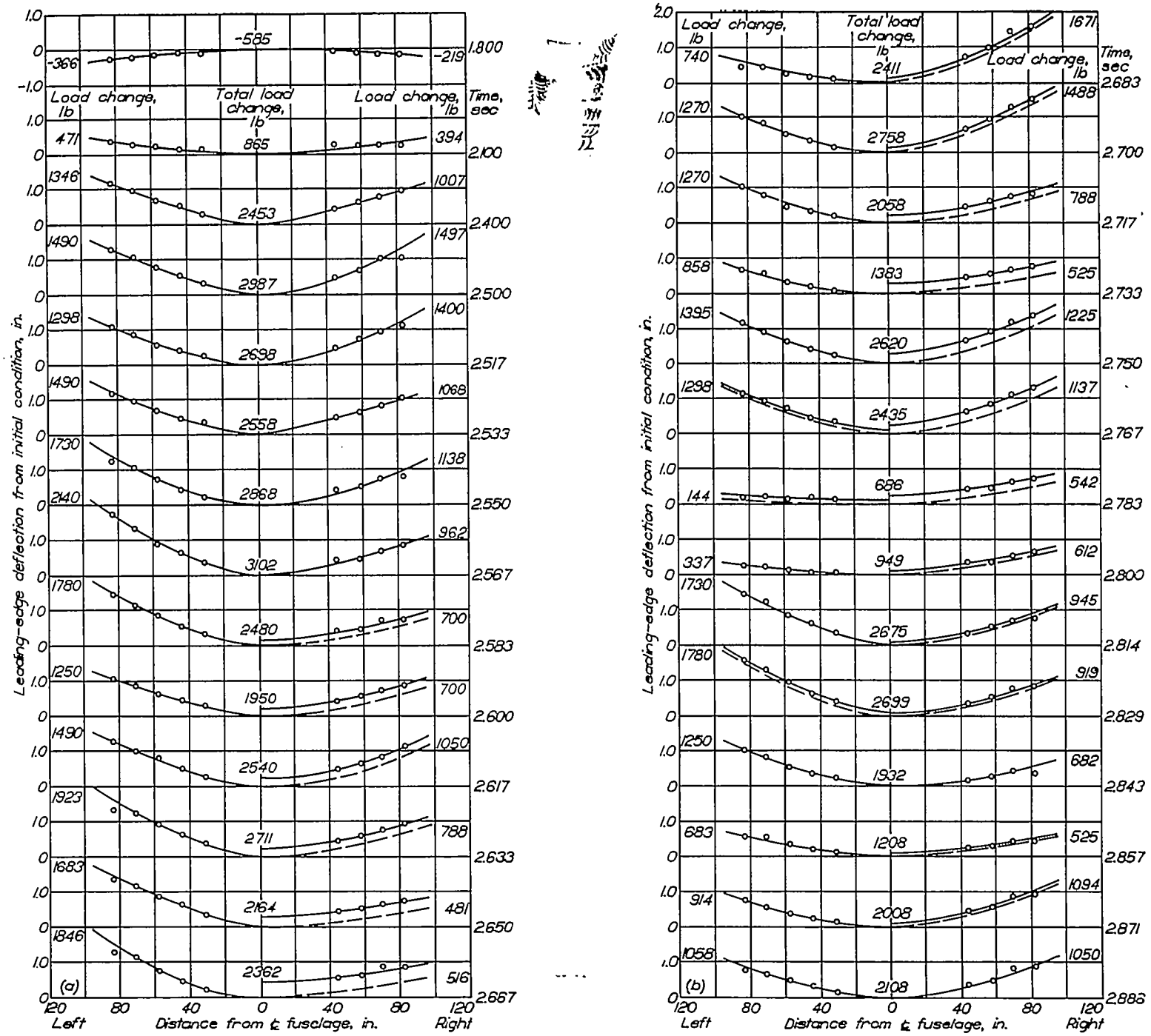

FIGURE 17.—Instantaneous beam diagrams of stabilizer obtained during a 4.2g pull-up to maximum lift. Run 2 of flight 24B.

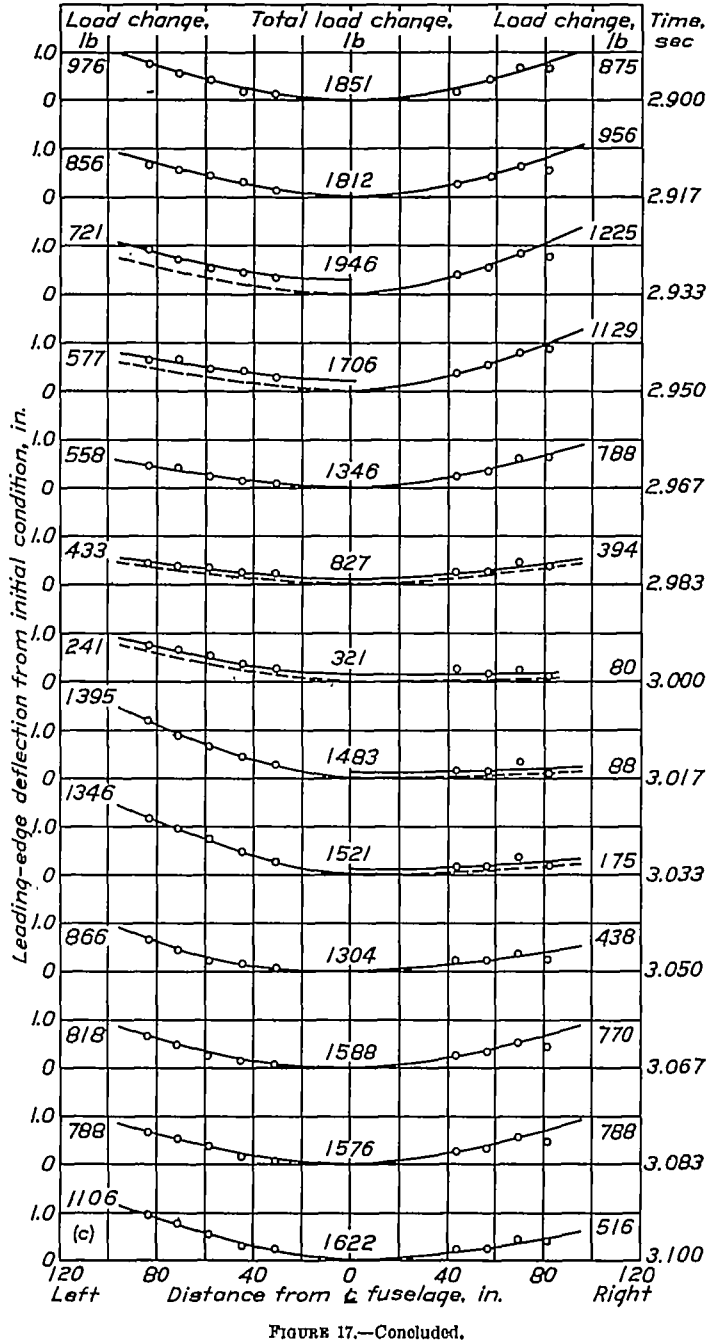

FIGURE 17.—Concluded.

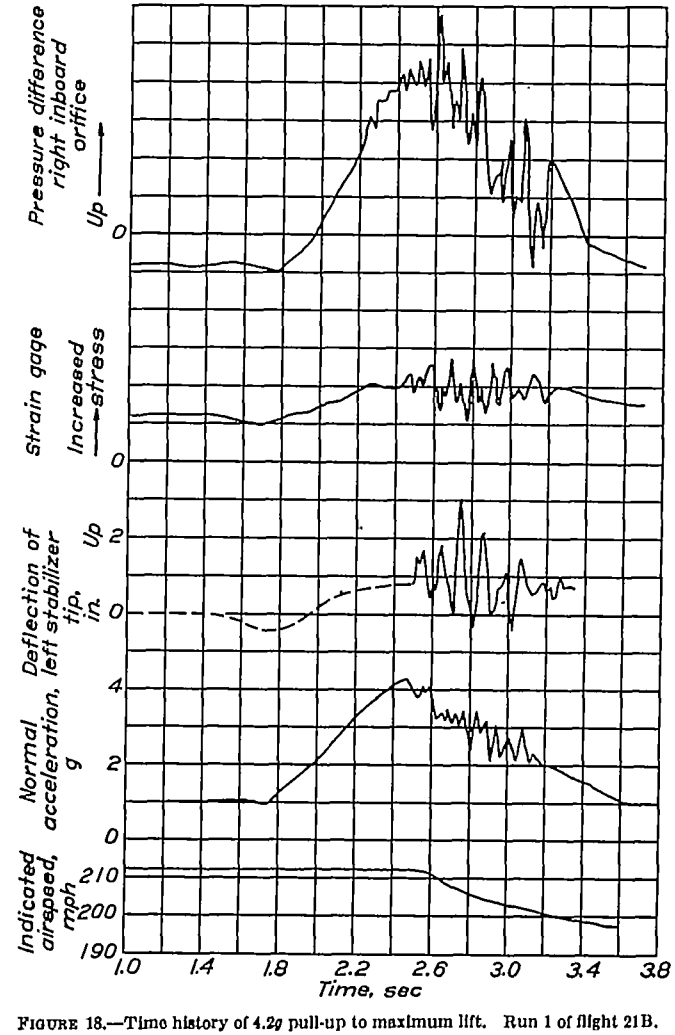

FIGURE 18.—Time history of 4.2g pull-up to maximum lift. Run 1 of flight 21B.

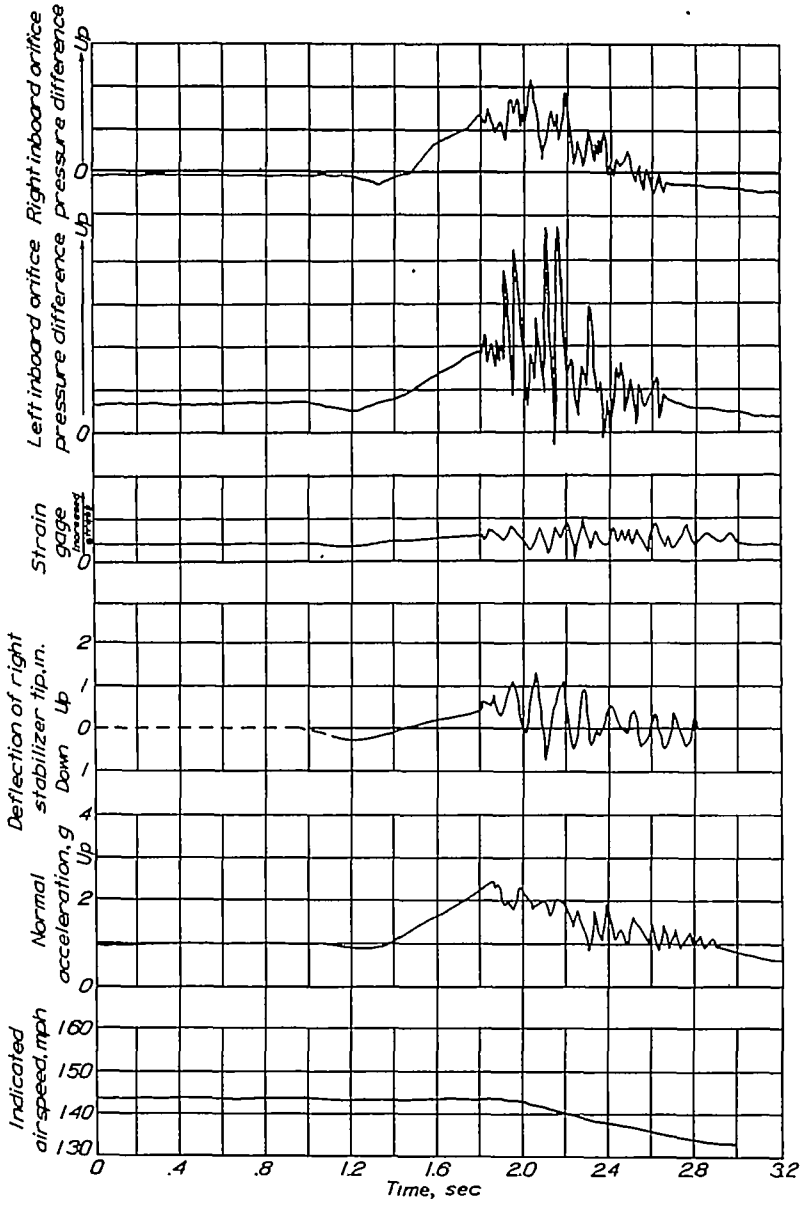

FIGURE 19.—Time history of a 2.4g pull-up to maximum lift. Run 1 of flight 24B.

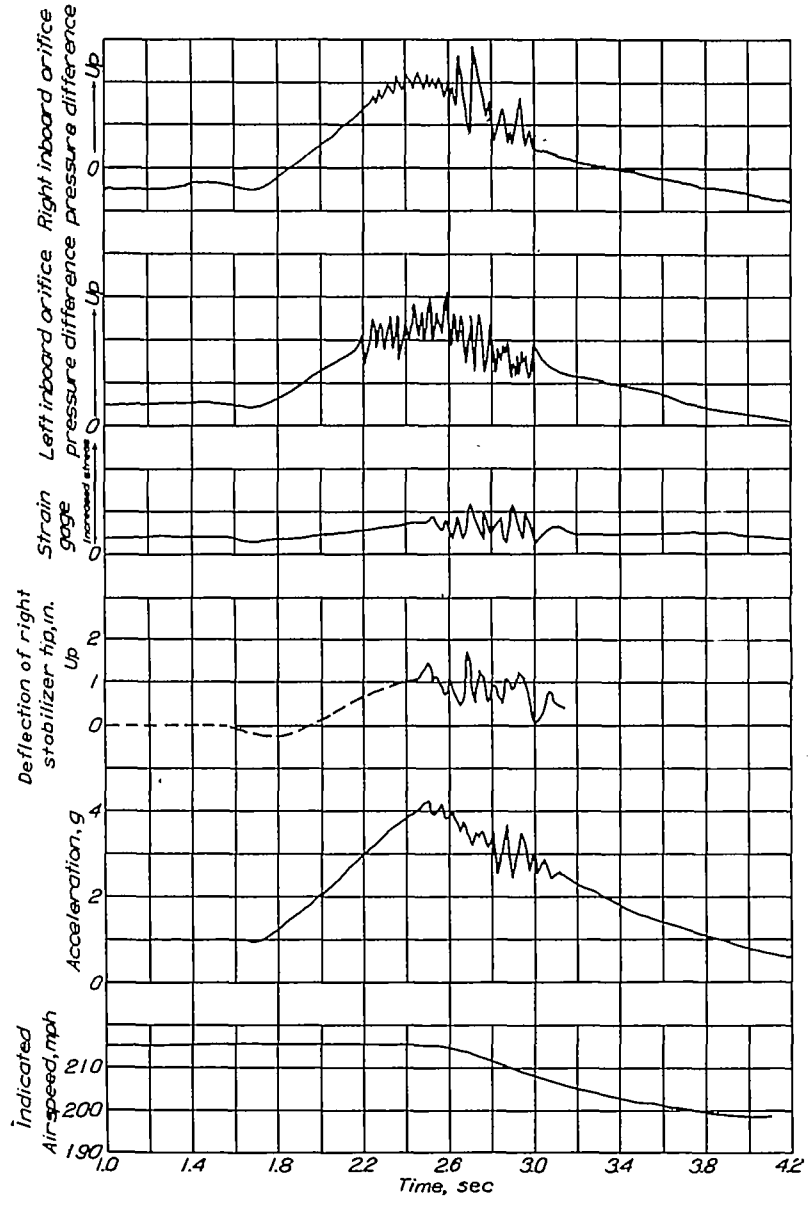

FIGURE 20.—Time history of a 4.2g pull-up to maximum lift. Run 2 of flight 24B.

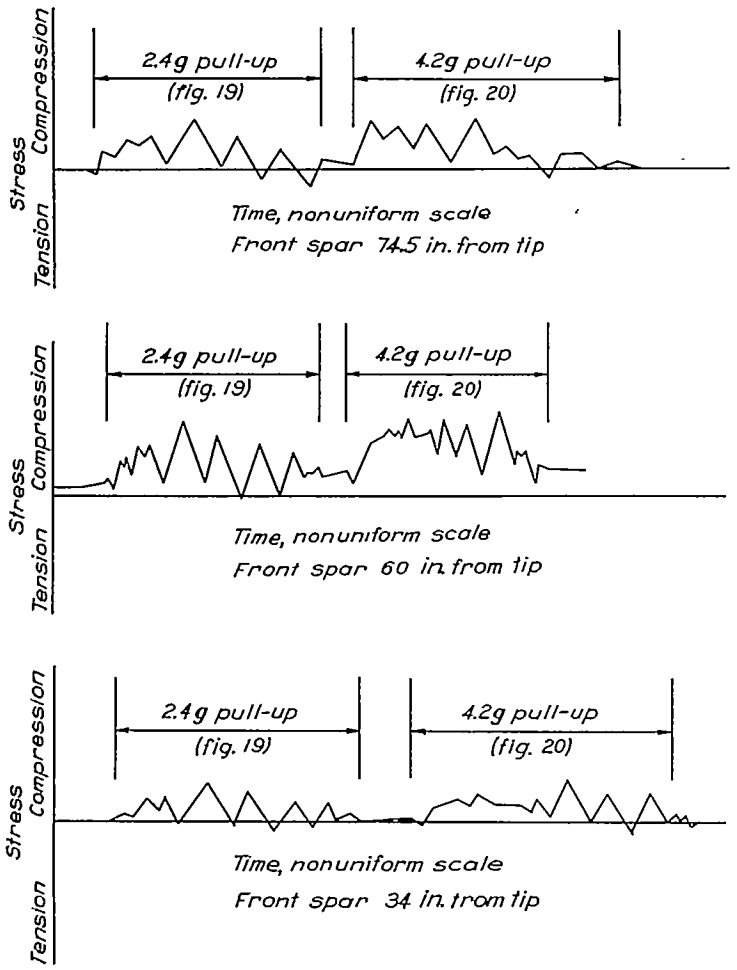

FIGURE 21.—Records from de Forest scratch-type strain gages for flight 24B. (Complete data for flight 24B are presented in figs. 19 and 20.)

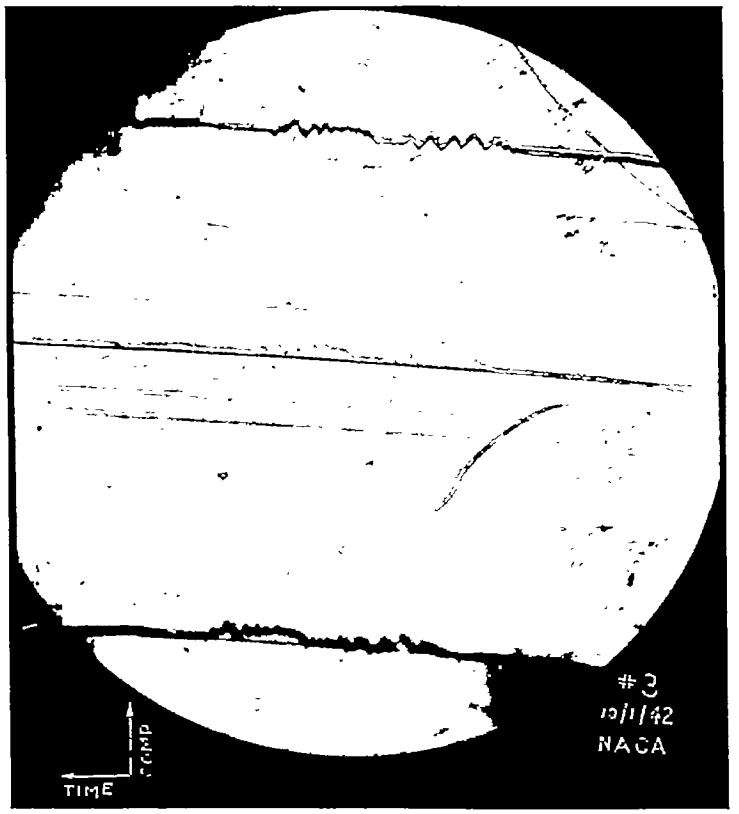

FIGURE 22.—Photomicrograph of a typical scratch-gage record. Gage located 60 inches from tip of stabilizer. Maneuvers: pull-up to 2.4g at 144 miles per hour and pull-ups to 4.2g at 214 miles per hour.

The conclusions to be drawn from the present tests are summarized as follows:

1. In abrupt pull-ups, the critical horizontal-tail loads were up loads and were substantially proportional to the maximum normal acceleration. For unstalled pull-ups, extrapolation of the test results shows that a total tail load of 5700 pounds would be experienced at an acceleration of 8g. Of this total tail load, about 1000 pounds would be due to the manipulation of the elevator during the pull-up.

2. In unstalled maneuvers with power on, the spanwise loading on the horizontal tail was unsymmetrical. About 800 pounds more up load was carried by the left stabilizer than by the right stabilizer. The magnitude of this dissymmetry was essentially independent of the normal acceleration. With power off, the dissymmetry was greatly reduced.

3. In pull-ups to the stall, an abrupt increase in the tail load occurred immediately after the stall of the wing. Data for the particular airplane tested indicate that load increments of the order of 100 percent of the load just prior to stalling may be obtained.

4. In stalled pull-up maneuvers, the tail was buffeted repeatedly by the turbulent flow from the stalled wing. The possibility of excessive stresses due to resonance in this condition was indicated.

LANGLEY MEMORIAL AERONAUTICAL LABORATORY,
NATIONAL ADVISORY COMMITTEE FOR AERONAUTICS,
LANGLEY FIELD, VA., *May 8, 1944.*

TABLE I.—SUMMARY OF PRESSURE-DISTRIBUTION DATA FOR UNSTALLED FLIGHT OBTAINED FROM TESTS OF A FIGHTER AIRPLANE

Flight and run	Pressure difference across tail, $\Delta p/q$				Normal-force coefficient, C_N				Indicated airspeed (mph)	Acceleration (g)	Elevator deflection from stabilizer, δ_e (deg)
	Left outboard	Left inboard	Right inboard	Right outboard	Left outboard	Left inboard	Right inboard	Right outboard			
14B 1	0.940	1.058	0.709	0.771	0.58	0.63	------	0.48	167	2.95	−4.0
14B 2	.875	.907	.755	.907	.53	.55	------	.58	188	3.53	−4.5
14B 3	.810	.812	.743	.801	.42	.41	------	.45	214	4.57	−8.0
14B *4	.527	.524	.409	.280	.38	.37	------	.17	261	4.59	−.5
15B 3	.807	.900	.650	.742	.42	.46	------	.42	169	2.98	−8.0
15B 4	.802	.786	.649	.764	.40	.38	------	.42	190.5	3.67	−9.5
15B 5	.775	.716	.538	.678	.44	.40	------	.40	218	4.41	−5.5
15B *6	.536	.523	.295	.311	.40	.39	------	.21	258	4.52	.5
18B 1	.990	1.148	.624	.604	.58	.68	------	.35	144	2.31	−5.5
18B 2	.865	.798	.736	.871	.49	.44	------	.55	190	3.77	−6.0
18B 3	.808	.858	.636	.740	.50	.52	------	.48	212	4.49	−4.0
18B 4	.567	.684	.117	.567	.35	.42	------	.36	108	1.05	−3.0
19B *1	.169	.088	−.162	−.112	.10	.03	------	.14	243	1.05	2.3
19B *1	.482	.454	.239	.287	.35	.33	------	.18	226	3.4	0
19B *9	.463	.471	.179	.161	.29	.28	------	.06	236	3.5	−2.7
24B 1	1.01	1.12	.745	1.04	.69	.77	------	.71	114	2.43	−.6
24B 2	.565	.674	.522	.786	.44	.51	------	.57	216	4.2	1.8

* Unstalled pull-ups or turns.